JSHC
Japan Society of
Histochemistry and Cytochemistry
Established 1959

Acta Histochem. Cytochem. 50 (2): 95–104, 2017
doi: 10.1267/ahc.17001

Profiles of Periglomerular Cells in the Olfactory Bulb of Prokineticin Type 2 Receptor-deficient Mice

Atsuko Kubo[1], Mitsugu Sujino[1], Koh-hei Masumoto[1], Atsuko Fujioka[1], Toshio Terashima[2], Yasufumi Shigeyoshi[1] and Mamoru Nagano[1]

[1]Department of Anatomy and Neurobiology, Kindai University Faculty of Medicine, 377–2 Ohnohigashi, Osaka-Sayama City, Osaka 589–8511, Japan and [2]Division of Anatomy and Developmental Neurobiology, Department of Cell Biology and Physiology, Kobe University Graduate School of Medicine, 7–5–1 Kusunoki-cho, Chuo-ku, Kobe 650–0017, Japan

Received January 5, 2017; accepted March 22, 2017; published online April 22, 2017

Both prokineticin receptor 2 (*pkr2*) and prokineticin 2 (*pk2*) gene-deficient mice have hypoplasia of the main olfactory bulb (MOB). This hypoplasia has been attributed to disruption of the glomerulus that is caused by loss of afferent projection from olfactory sensory neurons (OSN), and to the impaired migration of granule cells, a type of interneuron. In the present study, we examined whether migration of the second type of interneuron, periglomerular cells (PGC), is dependent on the *pkr2* expression by observing the localization of distinct subpopulations of PGC: calretinin (CR)-, calbindin (CB)- and tyrosine hydroxylase (TH)-expressing neurons. In the *Pkr2*$^{-/-}$ mice, the construction of the layered structure of the MOB was partially preserved, with the exception of the internal plexiform layer (IPL) and the glomerular layer (GL). In the outermost layer of the MOB, abundant CR- and CB-immunopositive neurons were observed in the hypoplastic olfactory bulb. In addition, although markedly decreased, TH-immunopositive neurons were also observed in the outermost cell-dense region in the *Pkr2*$^{-/-}$. The findings suggest that the migration of PGC to the MOB, as well as the migration from the core to the surface region of the MOB, is not driven by the PK2-PKR2 system.

Key words: periglomerular cell, calbindin, caltetinin, tyrosine hydroxylase, prokineticin

I. Introduction

The main olfactory bulb (MOB) gathers odor information delivered from olfactory sensory neurons (OSN), located in the olfactory epithelium, and relays this information to elsewhere in the brain via the olfactory tract. Generally, two types of interneurons exist in the MOB: periglomerular cells (PGC), which are localized in the glomerular layer (GL), and granule cells, which are found in the granule cell layer (GCL) [2, 7, 15]. Both of these interneuron types are generated not only during embryogenesis but also throughout postnatal life [2, 14]. In adulthood, interneurons are produced in the subventricular zone (SVZ) of the lateral ventricle and migrate to the MOB via the rostral migratory stream (RMS) [15, 16]. In terms of synaptic connectivity to axons of the OSN, PGC can be further subdivided into two types. Dopaminergic neurons represent type 1 PGC, which have synaptic connections with olfactory nerves, while calretinin (CR)- and calbindin (CB)-expressing neurons, having no synaptic connections to the olfactory nerves, are named type 2 PGC [10, 11].

Prokineticin 1 (PK1) and prokineticin 2 (PK2) are secreted bioactive proteins [13] that are ligands of two prokineticin receptors, such as PKR1 and PKR2 [17, 24]. Both *Pk2*-deficient (*Pk2*$^{-/-}$) and *Pkr2*-deficient (*Pkr2*$^{-/-}$) mice were found to exhibit hypoplastic MOB [20, 22, 23], mainly caused by a shrunken GCL and loss of the glomeru-

Correspondence to: Dr. Mamoru Nagano, Department of Anatomy and Neurobiology, Kindai University Faculty of Medicine, 377–2 Ohnohigashi, Osaka-Sayama City, Osaka 589–8511, Japan.
E-mail: m-nagano@med.kindai.ac.jp

lus in the GL [18, 23]. Although dysfunction in the migration of granule cells has been reported [20], whether there is a dysfunction in the migration of PGC from the SVZ of the lateral ventricles to the MOB in *Pkr2*$^{-/-}$ mice has not been fully investigated. Previous studies have demonstrated that the number of PGC expressing tyrosine hydroxylase (TH), a dopamine-synthesizing enzyme, was markedly decreased in the MOB of *Pkr2*$^{-/-}$ mice [12, 23]. In order to examine whether PGC retain the ability to migrate to the MOB in *Pkr2*$^{-/-}$ mice, we analyzed the layered structure of the MOB and observed distribution of three distinct subpopulations of PGC: CR- and CB-containing neurons, as well as dopaminergic neurons marked by TH, in the MOB of *Pkr2*$^{-/-}$ mice.

II. Materials and Methods

Experimental animals

The generation of *Pkr2*$^{-/-}$ was originally described in our previous report [18]. The background of the mice was originally C57BL/6 J, but, with the low survival ratio of neonates, the genetic background was changed to the ICR strain. The colony used in the present study was established by 11 backcrosses with Jcl:ICR mice (CLEA Japan, Tokyo). The resulting strain was subsequently maintained by interbreeding for at least 10 generations. Genotypes were determined using an established PCR method. Wild type (WT) and mutant adult mice (n = 3) at 12–15 weeks old were used for comparison. This study was performed in compliance with the Rules and Regulations of the Animal Care and Use Committee of Kindai University School of Medicine, and adhered to the Guide for the Care and Use of Laboratory Animals, Kindai University School of Medicine.

Tissue preparation and immunohistochemistry

Most of the method was used successfully in our previous studies [12, 27]. First, 12- to 15-week-old adult mice were deeply anesthetized and intracardially perfused with 4% paraformaldehyde (PFA) in 0.1 M phosphate buffer (PB) at pH 7.4. The brains were then removed and immersed in the same fixative for 24 hr at 4°C, and transferred to 20% sucrose in PB for 48 hr at 4°C. Brains were frozen and sectioned at 30 μm thickness in the sagittal plane of the entire MOB using a cryostat (Leica, Germany). Free-floating sections were rinsed several times with 0.02 M phosphate-buffered saline (PBS), pH 7.4, and incubated for 1 hr at 4°C in PBS containing 1% normal goat serum and 0.3% Triton X-100. They were then bleached for 30 min with 50% methanol containing 3% H_2O_2 and rinsed three times for 15 min each with PBS. The sections were incubated for 2 days at 4°C in the primary rabbit anti-CR (AB5054 Merck Millipore, Germany), diluted 1:5000, rabbit anti-CB (AB1778 Merck Millipore, Germany), diluted 1:4000 and mouse anti-TH antibodies (MAB318; Merck Millipore, Germany), diluted 1:4000 in PBS containing 0.3% Triton X-100. After rinsing with PBS, sections were incubated for 24 hr at 4°C in biotinylated anti-rabbit IgG or biotinylated anti-mouse IgG (Vectastain ABC kit; Vector Laboratories, Burlingame, CA, USA), diluted 1:1000 in PBS. They were then washed three times for 20 min each with PBS and incubated in avidin-biotin complex (Vectastain ABC kit) diluted 1:1000 in PBS for 24 hr at 4°C. After rinsing with PBS, the sections were washed with 0.05 M Tris-HCl buffer, pH 7.4, and treated with 0.035% diaminobenzidine (DAB) and 0.05 M Tris-HCl buffer in the presence of 0.003% hydrogen peroxide for 10–15 min at room temperature. After the DAB reaction, they were rinsed with 0.05 M Tris-HCl buffer three times (for 10 min each). Free-floating sections were mounted onto 1% gelatin-coated glass slides. After being air-dried, they were dehydrated with a graded series of ethanol rinses, immersed in xylene, and embedded in Entellan (Merck, Darmstadt, Germany).

The specificity of antibodies was shown in control experiments and by the consistent distribution of immunopositive neurons. The same experimental procedure without the first antibody did not show immunopositive staining. The same antibodies utilized in the present immunohistochemical studies have been used successfully in previous studies [26, 28] and the distribution of immunopositive neurons in the present study was consistent with previous studies [1, 4, 6, 21]. Further, Western blotting analysis using the antibodies demonstrated the antibodies bind to the protein with molecular weight corresponding to the proteins targeted by immunohistochemistry (data not shown). These findings suggest the feasibility of our present study showing the distribution of the antigens by immunohistochemistry.

Definition of lateral, middle and medial sections

The first to third slices of every six serial sections were stained with anti-CR, anti-CB and anti-TH antibodies. The most medial to the most lateral sections of the olfactory bulb were collected and a set of six serial sections showing RMS were regarded as “middle sections”, and six adjacent medial and lateral serial sections were called “medial sections” and “lateral sections” in the present study, respectively.

Statistical analysis

To compare the numbers of TH-, CB- and CR-immunopositive neurons, immunopositive neurons in GL of WT and outermost cell-dense portion *Pkr2*$^{-/-}$ mice in medial (med), middle (mid) and lateral (lat) sagittal sections of MOB were counted manually under a microscope (n = 3) and calculate cell density of each or total per 40,000 μm^2. Individual values were analyzed for significant differences using two-tailed Student’s t test.

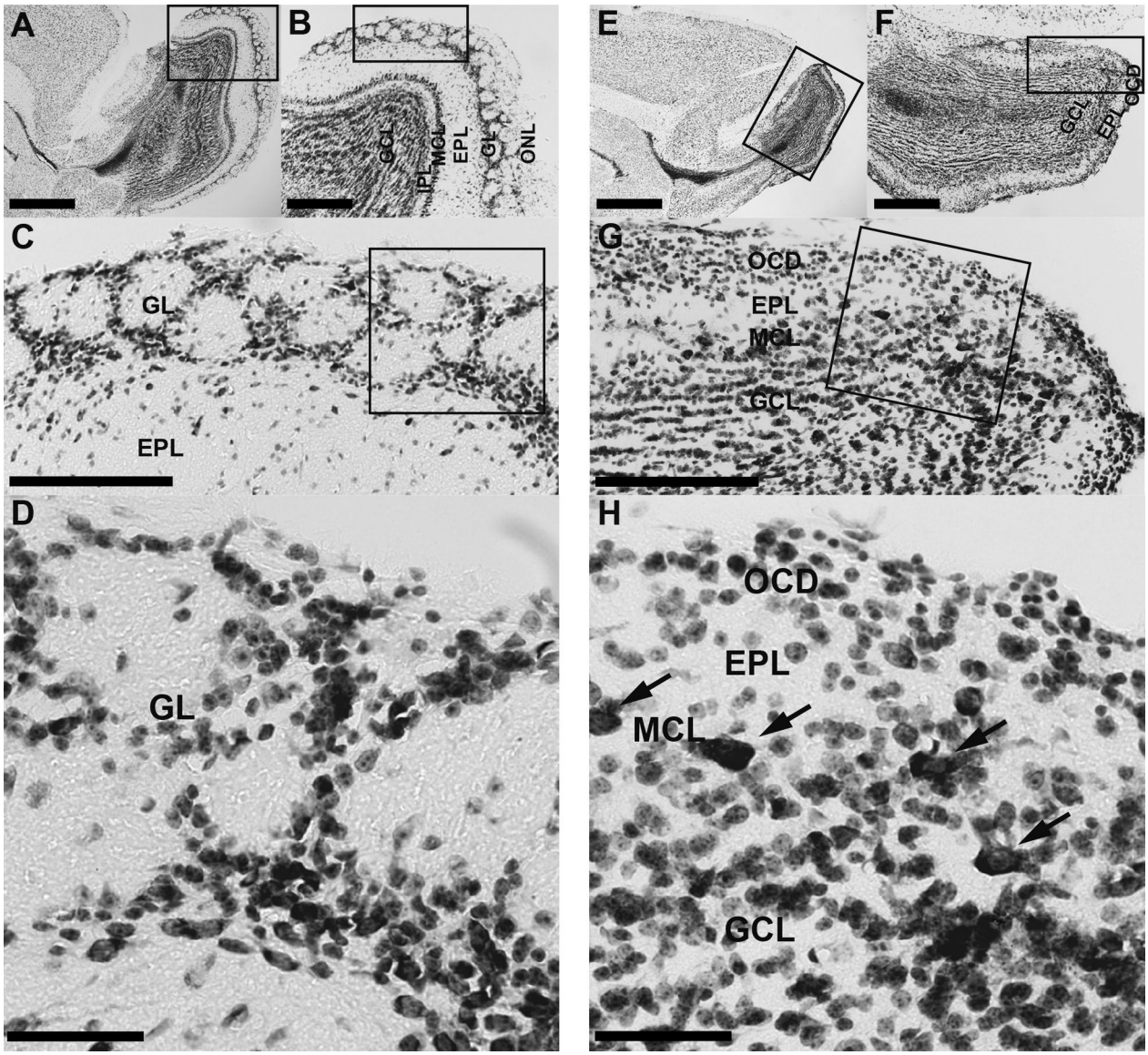

Fig. 1. Nissl-stained sagittal sections of the MOB in WT mice and *Pkr2*$^{-/-}$ mice. The rectangles indicate the areas magnified in the adjacent picture. Six layers, namely, olfactory nerve layer (ONL), glomerular layer (GL), external plexiform layer (EPL), mitral cell layer (MCL), internal plexiform layer (IPL) and granule cell layer (GCL), were recognized in the MOB of WT mice (**A–D**). In the *Pkr2*$^{-/-}$ (**E–H**), the ONL and IPL were not identified and the GCL was thinner than that in WT mice. Cell bodies were densely packed in the outermost layer of the MOB, which we named outermost cell-dense region (OCD). Mitral cells were located at the outer edge of the GCL (**H**, indicated by arrows). Bars = 1 mm (**A, E**); 400 μm (**B, F**); 200 μm (**C, G**); 50 μm (**D, H**).

III. Results

Layered structures of olfactory bulb in WT and Pkr2$^{-/-}$ *mice*

In the MOB of WT mice (Fig. 1A–D), six layers were distinguished by Nissl staining: olfactory nerve layer (ONL), GL, external plexiform layer (EPL), mitral cell layer (MCL), internal plexiform layer (IPL) and GCL [25]. The GL contained glomeruli that had a spherical structure surrounded by linearly arranged dense cell bodies (Fig. 1C, D). In *Pkr2*$^{-/-}$ mice, the MOB was much smaller than that of the WT mice (Fig. 1E, F) and the layered structure was partially preserved (Fig. 1E–H), as reported previously [18, 20]. The ONL was absent and densely packed cell bodies were identified in the outermost region of the MOB (Fig. 1G, H). Also, just inside of the outermost cell-dense region, an area with sparse cells compared with the EPL was seen (Fig. 1G, H). Further inside, large triangular cell bodies were densely situated in a narrow region (Fig. 1G, H), which formed the MCL, although the mitral cells were more scattered than those in WT mice. Inside the mitral cell layer, the IPL was not observed and the MCL continued to the inner layer, a wide cell-dense region corresponding to

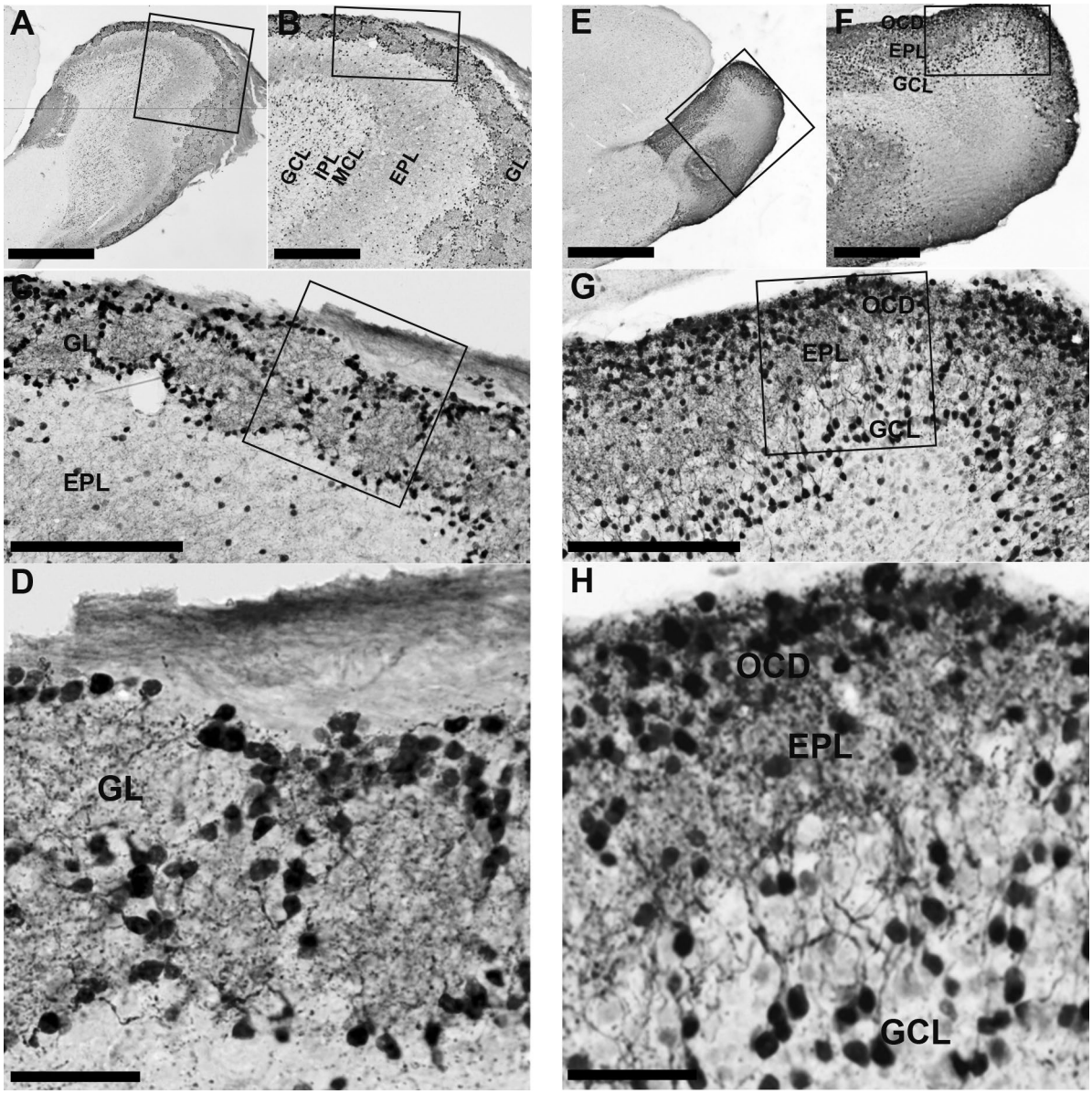

Fig. 2. Calretinin (CR)-immunopositive neurons in the OB of WT mice and *Pkr2*$^{-/-}$ mice. The rectangles indicate the areas magnified in the adjacent picture. In the MOB of WT mice, CR-immunopositive neurons were widely distributed through the glomerular layer (GL) to the granule cell layer (GCL). Strongly stained CR-immunopositive neurons were abundant in the GL, at the edge of the glomerulus (**A–D**). In the MOB of *Pkr2*$^{-/-}$ mice (**E–H**), strongly stained CR-immunopositive neurons were located mainly in the outermost cell-dense layer (OCD) and some were found in the cell-sparse region of the external plexiform layer (EPL) and GCL. MCL, mitral cell layer; IPL, internal plexiform layer. Bars = 1 mm (**A, E**); 400 μm (**B, F**); 200 μm (**C, G**); 50 μm (**D, H**).

the GCL. These observations suggest that the layered structure of the MOB is not completely disrupted but partially preserved.

Localization of CR-immunopositive neurons in the MOB of WT and Pkr2$^{-/-}$ *mice*

In WT mice, the GL contained many CR-immunopositive neurons that surrounded the glomeruli and strongly stained CR-immunopositive nerve fibers were abundant in regions both inside and outside of the glomeruli (Fig. 2A–D). In the EPL, immunopositive neurons were sparsely scattered and moderately stained nerve fibers were also sparsely localized (Fig. 2A–C). In the outer part of the GCL, dense CR-immunopositive neurons were present, but stained nerve fibers were sparse. The inner part of the GCL contained weakly labeled immunopositive neurons (Fig. 2A, B). In *Pkr2*$^{-/-}$ mice, intensely stained CR-immunopositive neurons and nerve fibers were densely packed in the outermost cell-dense region of the MOB. In the EPL, CR-immunopositive neurons were scarce, but immunopositive nerve fibers were densely distributed (Fig. 2E–H). Granule cells were strongly stained and situated in

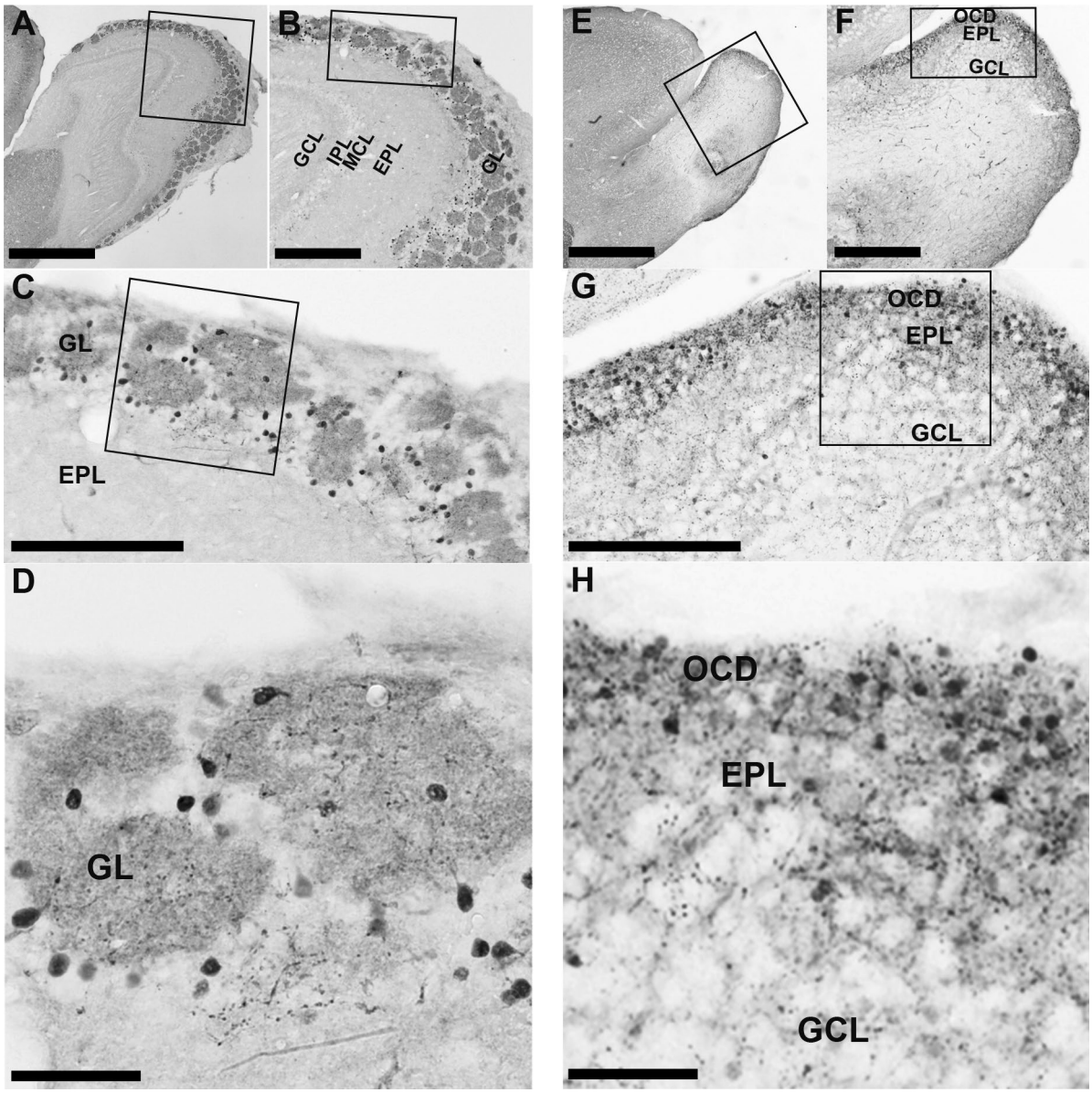

Fig. 3. Calbindin (CB)-immunopositive neurons in the OB of WT mice and *Pkr2*$^{-/-}$ mice. The rectangles indicate the areas magnified in the adjacent picture. In the MOB of *Pkr2*$^{-/-}$ mice, the majority of CB-immunopositive neurons were localized in the glomerular layer (GL) at the edge of the glomerulus (**A–D**). In *Pkr2*$^{-/-}$ mice, CB-immunopositive neurons were densely localized in mainly the outermost cell-dense region (OCD) and some cell-sparse area in the external plexiform layer (EPL) (**E–H**). MCL, mitral cell layer; IPL, internal plexiform layer; GCL, granule cell layer. Bars = 1 mm (**A, E**); 400 μm (**B, F**); 200 μm (**C, G**); 50 μm (**D, H**).

the outer region of the GCL (Fig. 2G, H). The inner region of the GCL contained weakly labeled immunopositive neurons and nerve fibers (Fig. 2E–G).

Localization of CB-immunopositive neurons in the MOB of WT and Pkr2*$^{-/-}$ *mice

In WT mice, most CB-immunopositive neurons were densely localized in the GL, surrounding the glomeruli (Fig. 3A–D). Strongly stained nerve fibers were also observed in the glomeruli. In the *Pkr2*$^{-/-}$ mice, immunopositive neurons and strongly stained immunopositive nerve fibers were observed in the outermost cell-dense region of the MOB (Fig. 3E–H). Further, weakly labeled neurons were observed in the cell-sparse region of the EPL and GCL, as was also seen in WT mice (Fig. 3E–H).

Localization of TH-immunopositive neurons in the MOB of WT and Pkr2*$^{-/-}$ *mice

In the MOB of WT mice, TH-immunopositive neurons were observed mainly in the GL. TH-immunopositive neurons were found surrounding the glomeruli, and strongly stained TH-immunopositive nerve fibers were widespread in the GL (Fig. 4A–D). In the EPL, a few strongly stained TH-immunopositive neurons and nerve fibers were

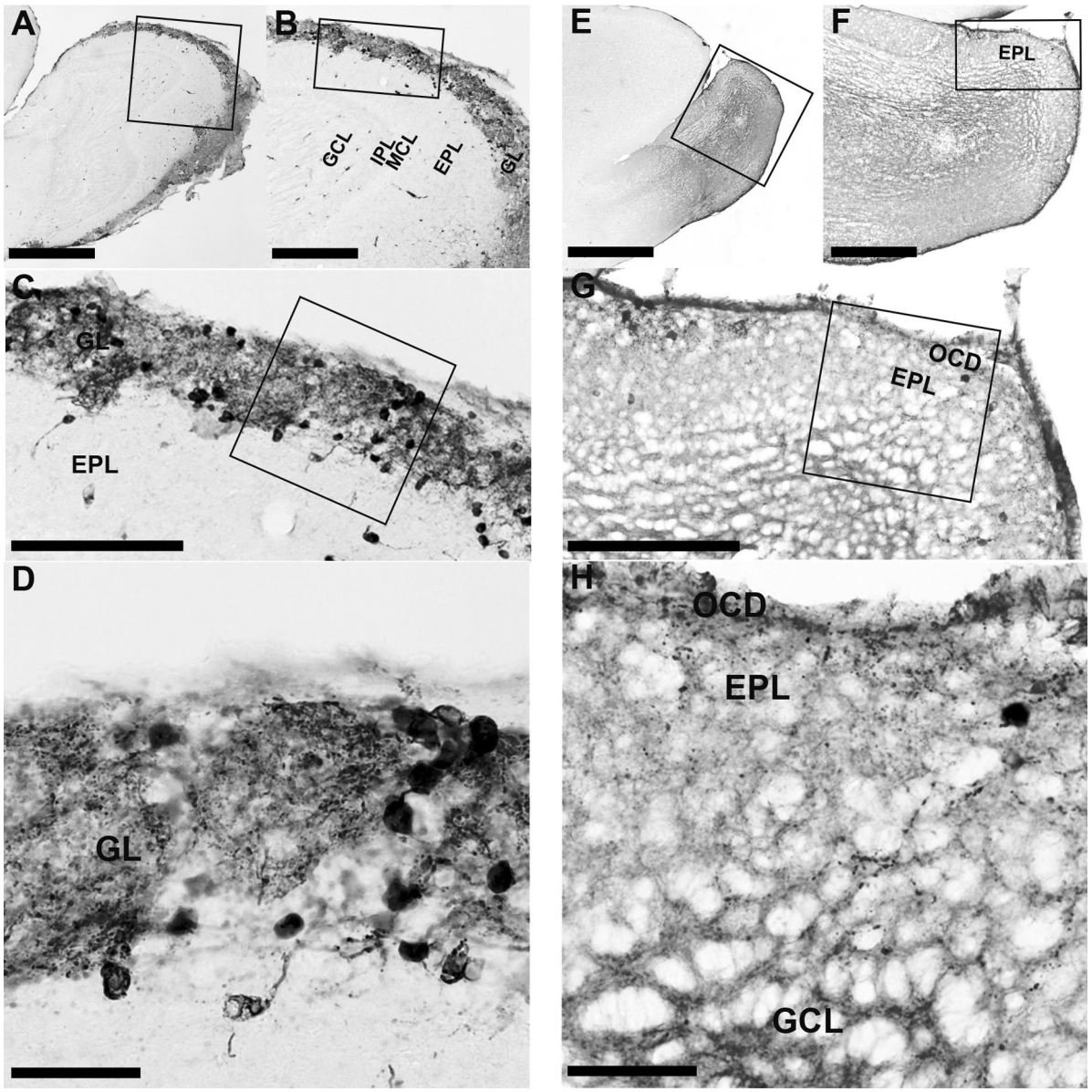

Fig. 4. TH-immunopositive neurons in the OB of WT mice and *Pkr2*$^{-/-}$ mice. The rectangles indicate the areas magnified in the adjacent picture. In the MOB of WT mice, TH-immunopositive neurons were distributed in the glomerular layer (GL) (**A–D**). In the mutant mice, a few TH-immunopositive neurons were localized in the outermost cell-dense region (OCD) (**E–H**). IPL, internal plexiform layer; MCL, mitral cell layer; EPL, external plexiform layer; GCL, granule cell layer. Bars = 1 mm (**A, E**); 400 μm (**B, F**); 200 μm (**C, G**); 50 μm (**D, H**).

observed (Fig. 4A–C). In the MOB of *Pkr2*$^{-/-}$ mice, TH-immunopositive neurons and nerve fibers were localized in the outermost cell-dense region (Fig. 4E–H). A few TH-immunopositive cells were observed in the MOB of *Pkr2*$^{-/-}$ compared with those in WT mice; the TH-immunopositive neurons and nerve fibers were markedly reduced in the MOB of *Pkr2*$^{-/-}$ (Fig. 4G, H, Fig. 5).

The number of TH-, CR- and CB-immunopositive neurons in MOB of WT and Pkr2$^{-/-}$ *mice*

To examine the difference in the manner of TH, CR and CB expression in PGC, the cell density of TH-, CR- and CB-immunopositive neurons of lateral, middle and medial sections (see Materials and Methods for the definition of each section) were counted in the MOB of WT and *Pkr2*$^{-/-}$ mice (Fig. 5). In WT mice, strongly labeled TH-, CR- and CB-immunopositive neurons were found surrounding the olfactory glomeruli in the GL, therefore, we measured the cell density in these mice by constructing rectangles that cover the GL and counted the number of immunopositive neurons (Fig. 5A–I, S–U, A'–I'). However, in *Pkr2*$^{-/-}$ mice, we measured the cell density by making rectangles that cover the outermost cell-dense region (Fig. 5J–R, V–X, J'–R'). The densities of CR- and CB-

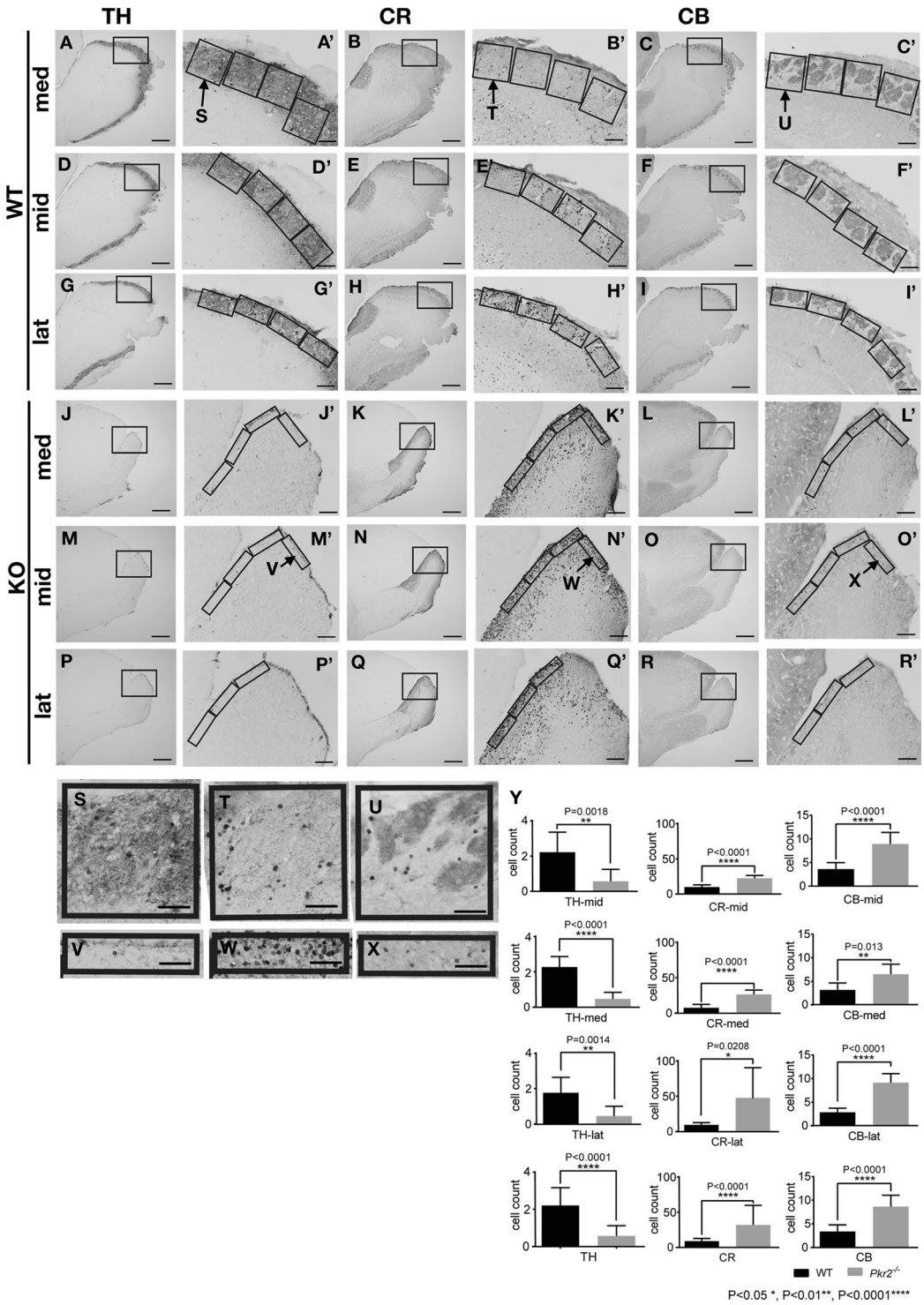

Fig. 5. The expression of TH-, CR- and CB-immunopositive neurons in lateral, middle and medial sections. TH-, CR- and CB-expressing neurons in medial (med), middle (mid) and lateral (lat) sagittal sections of the MOB in wild-type (WT) (**A–I', S, T, U**) and *Pkr2*$^{-/-}$ mice (KO) (**J–R', V, W, X**) (for the definitions of med, mid and lat sections, see Materials and Methods). The areas surrounded by rectangles in **A** to **R** are shown in **A'** to **R'** with higher magnification, respectively. The rectangles in the **A'** to **I'** covered the area from the surface to the inward edge of the GL. On the other hand, the rectangles in the **J'** to **R'** covered the area from the outer edge to the inner edge of the outermost cell-dense region. The number of TH-, CR- and CB-expressing neurons in the GL or outermost cell-dense region of the MOB of WT and *Pkr2*$^{-/-}$ mice in the rectangles (**A'–R'**) were counted and cell density of med, mid, lat and total of the three sections were calculated per 40,000 μm^2 (**Y**). In *Pkr2*$^{-/-}$, TH-immunopositive neurons were dramatically decreased in number in all sections we counted (**Y**). In contrast, CR- and CB-immunopositive neurons did not show a decrease in number, but showed an increase in number in *Pkr2*$^{-/-}$ (**Y**). Bars = 500 μm (**A–R**); 100 μm (**A'–R'**); 50 μm (**S–X**).

immunopositive neurons were significantly higher in the outermost cell-dense region of *Pkr2*$^{-/-}$ mice than those in the GL of WT mice (Fig. 5Y). In contrast, the density of TH-immunopositive cells in the outermost cell-dense region of *Pkr2*$^{-/-}$ mice was significantly lower than that in the GL of WT mice (Fig. 5Y).

IV. Discussion

With Nissl staining, we found that the layered structure of the MOB was partially preserved even in *Pkr2*$^{-/-}$ mice. The ONL, which forms the outermost layer of the MOB in WT mice, was absent in *Pkr2*$^{-/-}$ mice, as reported previously [18, 20]. Mitral cells were easily recognized by their large triangular cell bodies even in the disrupted MOB of *Pkr2*$^{-/-}$ mice. Although they were not aligned as well as in WT mice, we recognized a layer containing mitral cells in *Pkr2*$^{-/-}$ mice and regarded it as the MCL. The next outer layer of the MCL showed sparse cell bodies with rich neural fibers, indicating the layer corresponding to the EPL. In the outermost region of the MOB of *Pkr2*$^{-/-}$ mice, a cell-dense region was observed.

In *Pkr2*$^{-/-}$ mice, strongly stained dense CR- and CB-immunopositive neurons and a few TH-expressing neurons were localized in the outermost cell-dense region of the MOB. This observation suggests that the migration of PGC is independent of the PK2-PKR2 migratory system. The population of PGC consists of three distinct neuron subgroups, with each type expressing CR, CB, or TH, exclusively [10, 11]. In adulthood, PGC are produced in the SVZ of the lateral ventricle and migrate to the MOB via the RMS [15, 16] to the GL. In *Pkr2*$^{-/-}$ mice, CR- and CB- and TH-expressing neurons were localized in the outermost cell-dense region of the MOB. Therefore, in the MOB of *Pkr2*$^{-/-}$ mice, it is highly probable that the neurons expressing CR, CB, and TH in outermost cell dense layer were neurons that are comparable to PGC in WT mice. Then, it would be an interesting question whether the PGC-rich region belongs to the GL or the EPL. When the glomerulus of the MOB is absent, as was the case in *Pkr2*$^{-/-}$ mice, there is no landmark to determine the region corresponding to the GL in WT mice. The cluster of PGC did not support the existence of the GL since it is possible that the GL was completely lost and that PGC migrated to the outermost area of the EPL. Therefore, in *Pkr2*$^{-/-}$ mice, we could not determine whether PGC stayed at the EPL or migrated further to the GL.

In *Pkr2*$^{-/-}$ mice, CB-immunopositive neurons were mainly localized in the outermost cell-dense region of the MOB. On the other hand, CR-immunopositive neurons were localized in the outermost cell-dense region of the MOB, EPL and GCL. The distribution of the CR-immunopositive neurons in the layer other than the outermost cell-dense region is similar to that of WT mice. The observation suggests that PK2-PKR2 migratory system has little effect on the distribution of neurons expressing CR or CB in the MOB. To our knowledge, no reports have shown the functional difference between CR- and CB-expressing neurons. Therefore, the distinct functions of these neurons should be investigated further.

In *Pkr2*$^{-/-}$ mice, the ability of PGC to migrate to the final destination, the outermost cell-dense region, is a clear contrast to granule cells, which are supposed to be situated in the GCL, and their inability to migrate into the MOB of *Pkr2*$^{-/-}$ mice [23]. Migration of the granule cells expressing PKR2 into the GCL of MOB induced by PK2, a ligand of PKR2, functioning as a chemoattractant that is expressed in the MOB [20]. In contrast, our present observation suggests that CR- and CB-immunopositive cells do not utilize the PK2-PKR2 dependent migration system. Further, the presence of a few neurons expressing TH in the outermost cell-dense region of the MOB suggests that a subpopulation of dopaminergic neurons in the MOB still retain the ability to migrate to their final destination.

Neurons that synthesize dopamine are supposed to express TH, which is essential for the synthesis of dopa from L-tyrosine. Previous reports have demonstrated that, in the MOB, only PGC and superficial tufted cells express TH [10]. In the present study on *Pkr2*$^{-/-}$ mice, the number of TH-expressing neurons in the MOB were apparently decreased. Considering previous reports, there are two possible explanations for the decrease of TH-expressing neurons in *Pkr2*$^{-/-}$ mice. First, the population of neurons expressing TH failed to migrate to the MOB of *Pkr2*$^{-/-}$ mice. This situation might be similar to that of granule cells that failed to enter the MOB in *Pkr2*$^{-/-}$ mice [20]. It is possible that a few TH-immunopositive neurons remained in the MOB of *Pkr2*$^{-/-}$ mice are mostly superficial tufted cells. Second, the decrease in the number of TH-immunopositive neurons in PGC is attributable to the suppression of TH expression caused by deficits of afferent projection from OSN. Previous studies have demonstrated that deafferentation of projection of OSN to the MOB [3, 19] and naris closure [5, 8] lead to a marked decrease in the number of TH-expressing neurons in the GL. There was also a slight decrease in the number of neurons expressing the other dopamine-synthesizing enzyme, dopa decarboxylase [4]. Altogether, this suggests that dopaminergic neurons were present in the GL but ceased to express TH. Therefore, even in our present study, it is possible that suppression of odorant input caused by the absence of neural projection from OSN [18, 20] leads to a decrease in the expression of TH. Induction of TH in PGC is dependent on cFos induction, which acts via the AP-1 motif of promoter region of the TH [9]. Therefore, it is probable that the decrease of TH expression in PGC was caused by the absence of cFOS expression by deficit of afferent projection from OSN. The activation of PGC modifies the olfactory information with reciprocal synapses. In the mutant mice, the olfactory input was absent because of the loss of olfactory projection from the olfactory nerves. Therefore, it is unlikely that the loss of TH expression in PGC contributed to the modulation of

olfactory input. In addition to modulation of olfactory input, the other roles of dopaminergic PGC neurons are unknown thus far.

V. Abbreviations

CB, calbindin; CR, calretinin; EPL, external plexiform layer; GCL, granule cell layer; GL, glomerular layer; IPL, internal plexiform layer; MCL, mitral cell layer; MOB, main olfactory bulb; ONL, olfactory nerve layer; OSN, olfactory sensory neurons; PK1, prokineticin 1; PK2, Prokineticin 2; Pkr2$^{-/-}$, Pkr2-deficient; PGC, periglomerular cells; RMS, rostral migratory stream; SVZ, subventricular zone; TH, tyrosine hydroxylase; WT, wild type.

VI. Highlights

- The layered structure of the main olfactory bulb (MOB) of *Pkr2*$^{-/-}$ mice is partially preserved.
- CB, CR and TH-expressing PGC are localized in the outermost cell-dense region of the MOB of *Pkr2*$^{-/-}$ mice.
- PGC of the *Pkr2*$^{-/-}$ mice preserve the ability to migrate to the region close to the edge of the MOB.

VII. Acknowledgments

We thank Dr. Shun-Ichiro Matsumoto for kindly providing the *Pkr2* knockout mice. We also thank Ms. Emiko Kashima and Ms. Yayoi Yamanaka for their technical support. This research was supported by a Grant-in-Aid for Scientific Research from the Japanese Ministry of Education, Science, Sports and Culture of Japan. The authors declare no conflict of interest.

VIII. References

1. Alonso, J. R., Arevalo, R., Porteros, A., Brinon, J. G., Lara, J. and Aijon, J. (1993) Calbindin D-28K and NADPH-diaphorase activity are localized in different populations of periglomerular cells in the rat olfactory bulb. *J. Chem. Neuroanat.* 6; 1–6.
2. Altman, J. (1969) Autoradiographic and histological studies of postnatal neurogenesis. IV. Cell proliferation and migration in the anterior forebrain, with special reference to persisting neurogenesis in the olfactory bulb. *J. Comp. Neurol.* 137; 433–457.
3. Baker, H., Kawano, T., Margolis, F. L. and Joh, T. H. (1983) Transneuronal regulation of tyrosine hydroxylase expression in olfactory bulb of mouse and rat. *J. Neurosci.* 3; 69–78.
4. Baker, H., Kawano, T., Albert, V., Joh, T. H., Reis, D. J. and Margolis, F. L. (1984) Olfactory bulb dopamine neurons survive deafferentation-induced loss of tyrosine hydroxylase. *Neuroscience* 11; 605–615.
5. Baker, H., Morel, K., Stone, D. M. and Maruniak, J. A. (1993) Adult naris closure profoundly reduces tyrosine hydroxylase expression in mouse olfactory bulb. *Brain Res.* 614; 109–116.
6. Bastianelli, E., Okazaki, K., Hidaka, H. and Pochet, R. (1993) Neurocalcin immunoreactivity in rat olfactory bulb. *Neurosci. Lett.* 161; 165–168.
7. Carleton, A., Petreanu, L. T., Lansford, R., Alvarez-Buylla, A. and Lledo, P. M. (2003) Becoming a new neuron in the adult olfactory bulb. *Nat. Neurosci.* 6; 507–518.
8. Cho, J. Y., Min, N., Franzen, L. and Baker, H. (1996) Rapid down-regulation of tyrosine hydroxylase expression in the olfactory bulb of naris-occluded adult rats. *J. Comp. Neurol.* 369; 264–276.
9. Ghee, M., Baker, H., Miller, J. C. and Ziff, E. B. (1998) AP-1, CREB and CBP transcription factors differentially regulate the tyrosine hydroxylase gene. *Brain Res. Mol. Brain Res.* 55; 101–114.
10. Halasz, N., Johansson, O., Hokfelt, T., Ljungdahl, A. and Goldstein, M. (1981) Immunohistochemical identification of two types of dopamine neuron in the rat olfactory bulb as seen by serial sectioning. *J. Neurocytol.* 10; 251–259.
11. Kosaka, K. and Kosaka, T. (2007) Chemical properties of type 1 and type 2 periglomerular cells in the mouse olfactory bulb are different from those in the rat olfactory bulb. *Brain Res.* 1167; 42–55.
12. Kubo, A., Nagano, M., Sujino, M., Masumoto, K., Yamazaki, C., Terashima, T. and Shigeyoshi, Y. (2012) Profile of tyrosine hydroxylase-expressing neurons in the olfactory bulb of prokiniticin type 2 receptor-deficient mice during embryonic development. *Acta Med. Kinki Univ.* 37; 25–33.
13. Li, M., Bullock, C. M., Knauer, D. J., Ehlert, F. J. and Zhou, Q. Y. (2001) Identification of two prokineticin cDNAs: recombinant proteins potently contract gastrointestinal smooth muscle. *Mol. Pharmacol.* 59; 692–698.
14. Lledo, P. M., Merkle, F. T. and Alvarez-Buylla, A. (2008) Origin and function of olfactory bulb interneuron diversity. *Trends Neurosci.* 31; 392–400.
15. Lois, C. and Alvarez-Buylla, A. (1994) Long-distance neuronal migration in the adult mammalian brain. *Science* 264; 1145–1148.
16. Luskin, M. B. (1993) Restricted proliferation and migration of postnatally generated neurons derived from the forebrain subventricular zone. *Neuron* 11; 173–189.
17. Masuda, Y., Takatsu, Y., Terao, Y., Kumano, S., Ishibashi, Y., Suenaga, M., Abe, M., Fukusumi, S., Watanabe, T., Shintani, Y., Yamada, T., Hinuma, S., Inatomi, N., Ohtaki, T., Onda, H. and Fujino, M. (2002) Isolation and identification of EG-VEGF/prokineticins as cognate ligands for two orphan G-protein-coupled receptors. *Biochem. Biophys. Res. Commun.* 293; 396–402.
18. Matsumoto, S., Yamazaki, C., Masumoto, K. H., Nagano, M., Naito, M., Soga, T., Hiyama, H., Matsumoto, M., Takasaki, J., Kamohara, M., Matsuo, A., Ishii, H., Kobori, M., Katoh, M., Matsushime, H., Furuichi, K. and Shigeyoshi, Y. (2006) Abnormal development of the olfactory bulb and reproductive system in mice lacking prokineticin receptor PKR2. *Proc. Natl. Acad. Sci. U S A* 103; 4140–4145.
19. Nadi, N. S., Head, R., Grillo, M., Hempstead, J., Grannot-Reisfeld, N. and Margolis, F. L. (1981) Chemical deafferentation of the olfactory bulb: plasticity of the levels of tyrosine hydroxylase, dopamine and norepinephrine. *Brain Res.* 213; 365–377.
20. Ng, K. L., Li, J. D., Cheng, M. Y., Leslie, F. M., Lee, A. G. and Zhou, Q. Y. (2005) Dependence of olfactory bulb neurogenesis on prokineticin 2 signaling. *Science* 308; 1923–1927.
21. Parrish-Aungst, S., Shipley, M. T., Erdelyi, F., Szabo, G. and Puche, A. C. (2007) Quantitative analysis of neuronal diversity in the mouse olfactory bulb. *J. Comp. Neurol.* 501; 825–836.
22. Pitteloud, N., Zhang, C., Pignatelli, D., Li, J. D., Raivio, T., Cole, L. W., Plummer, L., Jacobson-Dickman, E. E., Mellon, P. L., Zhou, Q. Y. and Crowley, W. F., Jr. (2007) Loss-of-function mutation in the prokineticin 2 gene causes Kallmann syndrome

and normosmic idiopathic hypogonadotropic hypogonadism. *Proc. Natl. Acad. Sci. U S A* 104; 17447–17452.
23. Prosser, H. M., Bradley, A. and Caldwell, M. A. (2007) Olfactory bulb hypoplasia in Prokr2 null mice stems from defective neuronal progenitor migration and differentiation. *Eur. J. Neurosci.* 26; 3339–3344.
24. Soga, T., Matsumoto, S., Oda, T., Saito, T., Hiyama, H., Takasaki, J., Kamohara, M., Ohishi, T., Matsushime, H. and Furuichi, K. (2002) Molecular cloning and characterization of prokineticin receptors. *Biochim. Biophys. Acta* 1579; 173–179.
25. Switzer, R. C., de Olmos, J. and Heimer, L. (1985) Olfactory system. In "The rat nervous system", vol. 1, ed. by G. Paxinos, Academic Press, Australia, pp. 1–36.
26. Weihe, E., Depboylu, C., Schutz, B., Schafer, M. K. and Eiden, L. E. (2006) Three types of tyrosine hydroxylase-positive CNS neurons distinguished by dopa decarboxylase and VMAT2 co-expression. *Cell Mol. Neurobiol.* 26; 659–678.
27. Yamazaki, C., Nagano, M., Sujino, M., Kubo, A., Terashima, T., Ozawa, H. and Shigeyoshi, Y. (2012) Abnormal structures of olfactory bulb in prokineticin receptor 2 deficient mice with special references to layer specific neurotransmitter-expressing neurons. *Acta Med. Kinki Univ.* 37; 35–43.
28. Yoshihara, S., Omichi, K., Yanazawa, M., Kitamura, K. and Yoshihara, Y. (2005) Arx homeobox gene is essential for development of mouse olfactory system. *Development* 132; 751–762.